The Piezoresistive Effect in Top–Down Fabricated p-Type 3C-SiC Nanowires

Hoang-Phuong Phan, Toan Dinh, Takahiro Kozeki, Tuan-Khoa Nguyen, Afzaal Qamar, Takahiro Namazu, Nam-Trung Nguyen, and Dzung Viet Dao

***Abstract*— This letter reports on the piezoresistive effect of top–down fabricated 3C-SiC nanowires (NWs). Focused ion beam was utilized to create p-type 3C-SiC NWs from a 3C-SiC thin film with a carrier concentration of 5×10^{18} cm^{-3} epitaxially grown on a Si substrate. The as-fabricated NWs were then subjected to tensile strains varying from 0 to 280 $\mu\varepsilon$. Experimental data showed that the p-type 3C-SiC NWs possess a large gauge factor of 35, which is at least one order of magnitude larger than that of other hard materials, such as carbon nanotubes and graphene. This large gauge factor and the linear relationship between the relative resistance change and the applied strain in the SiC NWs indicate their potential for nanoelectromechanical systems sensing applications.**

***Index Terms*— Silicon carbide, piezoresistive effect, nanowires, NEMS sensors, focused ion beam.**

I. Introduction

PIEZORESISTIVE effect is one of the most commonly used sensing mechanisms in Micro Electro Mechanical Systems (MEMS) transducers, owing to its simple readout and compatibility with integrated circuits [1]–[6]. The piezoresistive effect in nano structures has attracted great attention as a means of device miniaturization [7]–[9]. For instance, a large number of studies have been carried out on silicon nanowires (SiNWs) – the most popular semiconductors used in MEMS. Applications of Si NW based piezoresistive sensors can be found in pressure sensors [10], flow sensors [12], accelerometers [11], and biomass detecting sensors [13].

Demands for electronics which can operate at high frequencies and high corrosion conditions have prompted the research on high stiffness materials to replace Si based counterparts. Thanks to their large Young's modulus (above 300 GPa), carbon based devices can offer higher resonance frequencies and Q-factors as compared to Si based devices [14]. The excellent mechanical properties also make carbon based materials suitable for extensive abrasion, such as the scanning tips of AFM (Atomic force Microscopy) based data storage systems [15]. The piezoresistive effect in CNTs [16], [17], graphene [18]–[20], and CNT yarns [21], [22] has also been investigated to develop niche sensing applications. The gauge factor of pure CNTs, CNT yarns, and graphene has been reported to be in the range of 0 to 10. To enhance the gauge factor of these materials, sophisticated structures such as CNT cross-links [23], graphene networks [24], [25], and back-gated CNT FETs [26] are required. More importantly, to integrate these materials with CMOS (Complementary Metal-Oxide Semiconductor) devices, additional processes such as exfoliation, sampling, and/or transferring are required [16], [20]. Therefore a wafer-scale high stiffness material which can be directly integrated with CMOS devices, and can offer a significant piezoresistive effect is preferable for ubiquitous mechanical sensors.

Single crystalline cubic silicon carbide (3C-SiC), a carbon based material, can solve the above-mentioned bottleneck, as it can be grown on a large scale Si substrate [27], [28]. This capability advances the fabrication of SiC based on the conventional MEMS process, and also makes 3C-SiC compatible with CMOS devices. The large energy band gap, and excellent physical properties have proved the feasibility of 3C-SiC in MEMS transducers such as strain, temperature, and optical sensors operating in harsh environments [29]–[31]. The piezoresistive effect in SiC NWs has also been reported recently [32]–[34]. However, most of these studies focused on bottom-up SiC NWs, while the piezoresistive effect of top-down fabricated SiC has not been fully understood. In addition, in the previous work on the piezoresistive effect in SiC NWs, external mechanical strains were locally induced into a certain point of SiC NWs [33], [34], while the effect of the uniaxial strain on the conductivity of SiC NWs has been rarely reported.

This letter presents the characterization of the piezoresistive effect of p-type 3C-SiC NWs, fabricated using a top-down process. The gauge factor of the SiC NWs under uniaxial strain was found to be 35. Taking the advantages of the compatibility with conventional MEMS processes and the capability of integrating with other CMOS devices, the as-fabricated SiC NWs on a Si substrate show their significant potential for NEMS mechanical sensors such as piezoresistive AFM, and self-sensing nano resonators.

II. Sample Preparation

Figure 1(a) shows the fabrication of the SiC NWs used in this study. Prior to the fabrication of SiC NWs, a 3C-SiC thin film with a thickness of 300 nm was grown on a Si wafer with a diameter of 300 mm using low pressure

Manuscript received April 29, 2016; revised June 5, 2016; accepted June 7, 2016. Date of publication June 9, 2016; date of current version July 22, 2016. This work was supported by the Australian Research Council through the Linkage Grant LP150100153. The review of this letter was arranged by Editor D. G. Senesky. *(Corresponding author: Hoang-Phuong Phan.)*

H.-P. Phan, T. Dinh, T.-K. Nguyen, A. Qamar, N.-T. Nguyen, and D. V. Dao are with the Queensland Micro- and Nanotechnology Centre, Griffith University, Nathan QLD 4111, Australia (e-mail: hoangphuong.phan@griffithuni.edu.au).

T. Kozeki is with the Department of Mechanical Engineering, University of Hyogo, Himeji 671-2280, Japan.

T. Namazu is with the Department of Mechanical Engineering, Aichi Institute of Technology, Toyota 470-0392, Japan.

Color versions of one or more of the figures in this letter are available online at http://ieeexplore.ieee.org.

Digital Object Identifier 10.1109/LED.2016.2579020

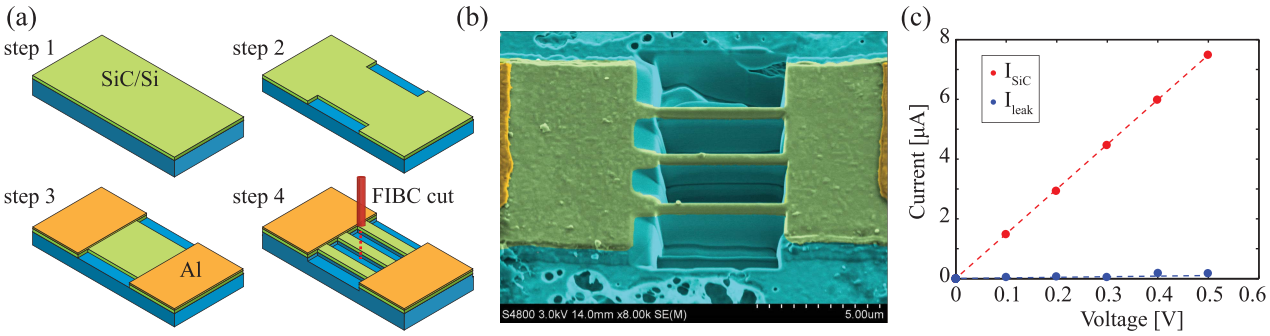

Fig. 1. (a) Fabrication of SiC NWs using a photolithography process and Focused Ion Beam; (b) SEM image of the as-fabricated SiC NWs in which the thickness, width, and length of the NWs were 300 nm, 300 nm and 5 μm, respectively. The SiC NWs were aligned along [110] direction; (c) The current-voltage of a SiC NWs array and the current leakage through the SiC/Si junction.

chemical vapor deposition. The details of the growth process can be found elsewhere [35], in which SiH_4 and C_3H_6 were employed as precursors. P-type 3C-SiC was formed where trimethylaluminum (TMAl) was the dopant. The properties of the SiC film has been reported in our previous studies [36]. The crystalline quality was characterized using high resolution transmission electro microscopy, indicating that crystal defect mainly distributed at the vicinity of the SiC/Si interface. As the thickness of the SiC film was 300 nm, which is much larger than the thickness of the high density defect layer, the influence of the defect layer on the electrical conductivity of SiC is insignificant [36]. Following the growth process, a thin layer of Al was deposited and patterned to create electrode pads. SiC micro patterns were then etched using Inductively Coupled Plasma. Next, SiC on Si strips with their lengths, widths and thicknesses of 60 mm, 8 mm, and 625 μm respectively, were diced from the SiC/Si wafer for the subsequent bending experiment. Finally, SiC NWs were formed using FIB (HITACHI FB 2200 ™), where gallium ion beam (Ga^+) was used to bombard the target material [37]. The applied voltage and DC current of the FIB process were 40 kV and 0.07 nA, respectively. Figure 1(b) illustrates the SEM image of a 3C-SiC NWs array. The dimensions of each SiC NW are 300 nm $\times$ 300 nm $\times$ 5 μm.

III. Results

The electrical properties of the SiC film were characterized using a hot probe technique [38]. The polarization of the output voltage in the hot probe measurement indicated that the grown film was p-type SiC. The carrier concentration in the p-type 3C-SiC film was found to be in a range of 5×10^{18} cm^{-3}. The current-voltage characteristic of the as-fabricated SiC NWs was investigated using an Agilent 2722A™ power supply. The linear relationship between the applied voltage and measured current indicates that a good Ohmic contact was formed between the Al electrodes and the SiC NWs resistors, Fig. 1(c). Additionally, utilizing the four-points measurement method, the contact resistance was found to be below 100 Ω, which is negligible compared to the resistance of the SiC NWs. Additionally, the leakage current from the function layer (SiC) to the substrate (Si) was also explored, showing a small leakage of 20 nA at an applied voltage of 0.5 V. The current leakage was much smaller than

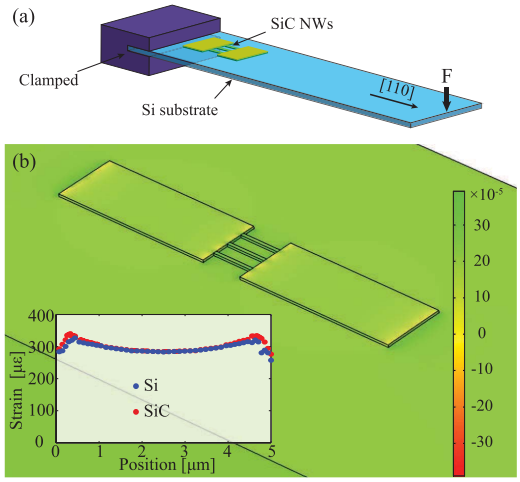

Fig. 2. (a) Schematic sketch of the bending experiment. The distance of from the SiC NWs to the free end of the Si cantilever is 48 mm, which is significantly longer than the length of the SiC NWs (5 μm). (b) Finite element analysis (FEA) results of the strain induced into SiC NWs using the bending beam method. Inset: A comparison between the strain induced into the SiC NWs and that of the top surface of the Si substrate.

the current flowing in the SiC NWs due to the discontinuity of the energy band in SiC and Si. The large energy difference between the top valance bands of SiC ($E_v = 6.9$ eV) and Si ($E_v = 5.2$ eV) causes a large potential barrier of $\Delta E_v = 1.7$ eV at the SiC/Si heterojunction. This potential barrier prevents holes from flowing across the junction. This result indicates that the low-doped Si substrate ($N_a = 10^{14}$ cm^{-3}) did not contribute to the measured piezoresistance of the SiC NWs.

Figure 2(a) shows the schematic of the bending beam method which was applied to induce strains into the as-fabricated SiC NWs. In this experiment, the above-mentioned SiC/Si strip was fixed in one side using a metal clamp. The other free side was deflected downward by applying different loads. As the distance from the SiC NWs to the free end of the beam was 48 mm, which is much longer than the length of the SiC NWs, the external strain was almost uniformly induced into the SiC NWs. Numerical calculation of the applied strain was then carried out, using the bilayer model which has been widely employed in piezoelectric actuators [39]. Accordingly, because the thickness of the top layer (300 nm) was much smaller than that of the bottom layer (625 μm Si), the external

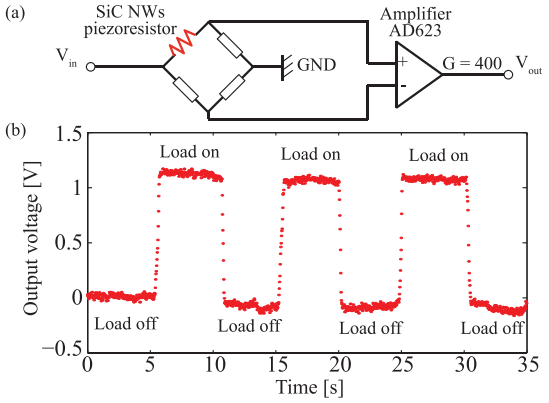

Fig. 3. (a) The Wheastone bridge and amplifier circuit; (b) The output voltage of a SiC NWs array under an applied tensile strain of 280 $\mu\varepsilon$ for three bending cycles.

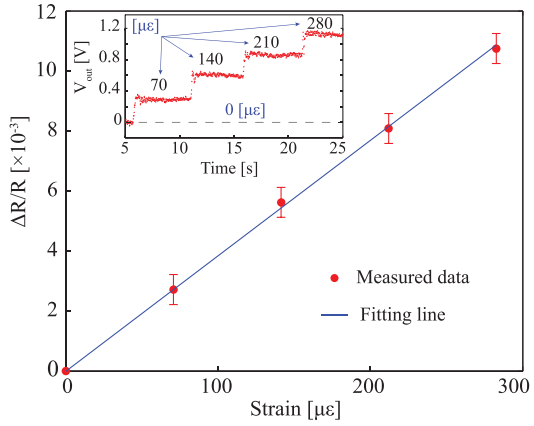

Fig. 4. The linear relationship between the relative resistance change ($\Delta R/R$) of a SiC NWs array against tensile strain varying from 0 to 280 $\mu\varepsilon$. Inset: the incrementation of the output voltage (V_{out}) with increasing applied strains.

strain was estimated to be approximately 100% transmitted from the top surface of the Si substrate to the SiC NWs [40]. Therefore, the strain induced into the SiC NWs can be calculated using the equation: $\varepsilon = 6Fl/(E\omega t^2)$, where F is the applied force to the free end of the Si beam, while E, l, ω, and t are Young's modulus, the length, the width, and the thickness of the Si beam, respectively. The strains applied to the SiC NWs were also estimated using finite element analysis, in which the Young's moduli of SiC and Si were 330 GPa and 169 GPa, respectively. The simulation results employing COMSOL Multiphysics™ was in solid agreement with the numerical calculation, indicating that the strain of SiC NWs was almost the same as that of the Si substrate, Fig. 2(b). In addition, the strain was slightly higher at the connecting area between the nanowires and electrode pads. This result is considered to be caused by the difference between the width of the electrode pads and that of the SiC NWs. However, this high strain only locally distributed at the connecting area; therefore it did not significantly change the average strain induced into the SiC NWs. Consequently, for applied loads varying from 0 to 0.4 N, the induced strains were found to be in the range of 0 to 280 $\mu\varepsilon$.

To measure the piezoresistive effect, the resistance change of the SiC NWs was converted into a voltage signal using a Wheatstone bridge and an op-amplifier (Analog Devices™ AD623), Fig. 3(a). The relationship between the relative resistance change ($\Delta R/R$) and the measured output voltage (V_o) is :

$$V_o = \frac{V_i}{4}\frac{\Delta R}{R}G \tag{1}$$

where $V_i = 1\ V$ is the supplied voltage of the Wheatstone bridge, and $G = 400$ is the gain of the op-amplifier. The output voltages were measured and recorded using an Oscilloscope during the bending experiment. Figure 3(b) shows the output voltage of the SiC NWs at an applied strain of 280 $\mu\varepsilon$. The repeatability of the output voltage against an external mechanical strain was also confirmed after several bending cycles. The inset in Fig. 4 presents the output voltages of the bridge at different applied strains. Evidently, the output voltage increased with increasing mechanical strains. Subsequently, the relative resistance change ($\Delta R/R$) was calculated using Eq. 1 and plotted against the applied strains, Fig. 4. Evidently, the relative resistance change has a linear relationship with the applied strains. Consequently, the gauge factor ($GF = (\Delta R/R)/\varepsilon$) of the SiC NWs was found to be 35.

The gauge factor found in the SiC NWs was much larger than that of other hard materials such as pure CNTs, and graphene. The piezoresistive effect in p-type 3C-SiC NWs can be qualitatively explained using the valance band modification under strain [33]. As such, an external mechanical strain causing the shift and warping in the heavy hole and light hole bands. As a result, the major carriers (holes) will redistribute in these two bands, following the rule that hole will fill up the lower energy first. Consequently, the redistribution of the holes will change the hole effective mass, as well as their mobility, leading to a change in the resistance of SiC NWs. On the other hand, the piezoresistive effect of pure CNTs and graphene is similar to metal, being mainly caused by the change in geometrical dimensions [20]. The gauge factor of our top-down fabricated NWs is also comparable to that of bottom up NWs characterized using a local point-strain [33], [34]. In addition, as the common strain gauges aim at measuring uniaxial strains, our finding in the piezoresistance of SiC NWs under uniaxial strain is significant for designing SiC NWs based strain sensors.

IV. Conclusion

In conclusion, this work reports on the piezoresistive effect in top-down fabricated SiC NWs for mechanical sensing applications. The compatibility with the MEMS photolithography process of the SiC NWs fabricated from SiC on Si wafer demonstrates its potential for mass production as well as suitability for the integration with CMOS devices. Additionally, the significant piezoresistive effect with a gauge factor of 35 found in the p-type 3C-SiC NWs also proved the feasibility of using this new platform for NEMS sensors.

References

[1] A. A. Barlian, W.-T. Park, J. R. Mallon, A. J. Rastegar, and B. L. Pruitt, "Review: Semiconductor piezoresistance for microsystems," *Proc. IEEE*, vol. 97, no. 3, pp. 513–552, Mar. 2009, doi: 10.1109/JPROC.2009.2013612.

[2] N. Minh-Dung, P. Hoang-Phuong, K. Matsumoto, and I. Shimoyama, "A sensitive liquid-cantilever diaphragm for pressure sensor," in *Proc. IEEE 26th Int. Conf. MEMS*, Taipei, Taiwan, Jan. 2013, pp. 617–620, doi: 10.1109/MEMSYS.2013.6474317.

[3] D. V. Dao, T. Toriyama, J. Wells, and S. Sugiyama, "Six-degree of freedom micro force-moment sensor for application in geophysics," in *Proc. 15th Int. Conf. IEEE MEMS*, Las Vegas, NV, USA, Jan. 2002, pp. 312–315, doi: 10.1109/MEMSYS.2002.984265.

[4] T.-V. Nguyen, M.-D. Nguyen, H. Takahashi, K. Matsumoto, and I. Shimoyama, "Viscosity measurement based on the tapping-induced free vibration of sessile droplets using MEMS-based piezoresistive cantilevers," *Lap Chip*, vol. 15, no. 18, pp. 3670–3676, 2015, doi: 10.1039/C5LC00661A.

[5] J. Bi, G. Wei, M. Shang, F. Gao, B. Tang, and W. Yang, "Carrier transport in graphite/Si_3N_4-nanobelt/PtIr Schottky barrier diodes," *Appl. Phys. Lett.*, vol. 105, no. 19, p. 191604, 2014, doi: 10.1063/1.4901821.

[6] J. Bi, G. Wei, M. Shang, F. Gao, B. Tang, and W. Yang, "Piezoresistance in Si_3N_4 nanobelts: Toward highly sensitive and reliable pressure sensors," *J. Mater. Chem. C*, vol. 2, no. 47, pp. 10062–10066, 2014, doi: 10.1039/C4TC01810A.

[7] R. He and P. Yang, "Giant piezoresistance effect in silicon nanowires," *Nature Nanotechnol.*, vol. 1, pp. 42–46, Oct. 2006, doi: 10.1038/nnano.2006.53.

[8] H.-P. Phan, T. Kozeki, T. Dinh, T. Fujii, A. Qamar, Y. Zhu, T. Namazu, N.-T. Nguyen, and D. V. Dao, "Piezoresistive effect of p-type silicon nanowires fabricated by a top-down process using FIB implantation and wet etching," *RSC Adv.*, vol. 5, no. 100, pp. 82121–82126, 2015, doi: 10.1039/C5RA13425K.

[9] K. Winkler, E. Bertagnolli, and A. Lugstein, "Origin of anomalous piezoresistive effects in VLS grown Si nanowires," *Nano Lett.*, vol. 15, no. 3, pp. 1780–1785, 2015, doi: 10.1021/nl5044743.

[10] C. J. Huang, C. H. Yang, C. Y. Hsueh, J. H. Lee, Y. T. Chang, and S. C. Lee, "Stress effects on self-aligned silicon nanowire junctionless field-effect transistors," *IEEE Electron Device Lett.*, vol. 32, no. 9, pp. 1194–1196, Sep. 2011, doi: 10.1109/LED.2011.2159772.

[11] L. Lou, W.-T. Park, S. Zhang, L. S. Lim, D.-L. Kwong, and C. Lee, "Characterization of silicon nanowire embedded in a MEMS diaphragm structure within large compressive strain range," *IEEE Electron Device Lett.*, vol. 32, no. 12, pp. 1764–1766, Dec. 2011, doi: 10.1109/LED.2011.2169931.

[12] S. Zhang, L. Lou, and C. Lee, "Piezoresistive silicon nanowire based nanoelectromechanical system cantilever air flow sensor," *Appl. Phys. Lett.*, vol. 100, no. 2, p. 023111, 2012, doi: 10.1063/1.3675878.

[13] R. He, X. L. Feng, M. L. Roukes, and P. Yang, "Self-transducing silicon nanowire electromechanical systems at room temperature," *Nano Lett.*, vol. 8, no. 6, pp. 1756–1761, 2008, doi: 10.1021/nl801071w.

[14] A. R. Kermany, G. Brawley, N. Mishra, E. Sheridan, W. P. Bowen, and F. Iacopi, "Microresonators with *Q*-factors over a million from highly stressed epitaxial silicon carbide on silicon," *Appl. Phys. Lett.*, vol. 104, no. 8, p. 081901, 2014, doi: 10.1063/1.4866268.

[15] M. A. Lantz, B. Gotsmann, P. Jaroenapibal, T. D. B. Jacobs, S. D. O'Connor, K. Sridharan, and R. W. Carpick, "Wear-resistant nanoscale silicon carbide tips for scanning probe applications," *Adv. Funct. Mater.*, vol. 22, no. 8, pp. 1639–1645, 2012, doi: 10.1002/adfm.201102383.

[16] M. A. Cullinan and M. L. Culpepper, "Carbon nanotubes as piezoresistive microelectromechanical sensors: Theory and experiment," *Phys. Rev. B*, vol. 82, no. 11, p. 115428, 2010, doi: 10.1103/PhysRevB.82.115428.

[17] N. Yang, X. Chen, T. Ren, P. Zhang, and D. Yang, "Carbon nanotube based biosensors," *Sens. Actuators B, Chem.*, vol. 207, pp. 690–715, Feb. 2015, doi: 10.1016/j.snb.2014.10.040.

[18] A. D. Smith, F. Niklaus, A. Paussa, S. Vaziri, A. C. Fischer, M. Sterner, F. Forsberg, A. Delin, D. Esseni, P. Palestri, M. Ostling, and M. C. Lemme, "Electromechanical piezoresistive sensing in suspended graphene membranes," *Nano Lett.*, vol. 13, no. 7, pp. 3237–3242, 2013, doi: 10.1021/nl401352k.

[19] X. He, L. Gao, N. Tang, J. Duan, F. Mei, H. Meng, F. Lu, F. Xu, X. Wang, X. Yang, W. Ge, and B. Shen, "Electronic properties of polycrystalline graphene under large local strain," *Appl. Phys. Lett.*, vol. 104, no. 24, p. 243108, 2014, doi: 10.1063/1.4883866.

[20] S.-E. Zhu, M. K. Ghatkesar, C. Zhang, and G. C. A. M. Janssen, "Graphene based piezoresistive pressure sensor," *Appl. Phys. Lett.*, vol. 102, no. 16, p. 161904, 2013, doi: 10.1063/1.4802799.

[21] J. L. Abot, T. Alosh, and K. Belay, "Strain dependence of electrical resistance in carbon nanotube yarns," *Carbon*, vol. 70, pp. 95–102, Apr. 2014, doi: 10.1016/j.carbon.2013.12.077.

[22] A. A. Obaid, D. Heider, and J. W. Gillespie, Jr., "Investigation of electro-mechanical behavior of carbon nanotube yarns during tensile loading," *Carbon*, vol. 93, pp. 731–741, Nov. 2015, doi: 10.1016/j.carbon.2015.05.091.

[23] S. Ryu, P. Lee, J. B. Chou, R. Xu, R. Zhao, A. J. Hart, and S.-G. Kim, "Extremely elastic wearable carbon nanotube fiber strain sensor for monitoring of human motion," *ACS nano*, vol. 9, no. 6, pp. 5929–5936, 2015, doi: 10.1021/acsnano.5b00599.

[24] X. Li, R. Zhang, W. Yu, K. Wang, J. Wei, D. Wu, A. Cao, Z. Li, Y. Cheng, Q. Zheng, R. S. Ruoff, and H. Zhu, "Stretchable and highly sensitive graphene-on-polymer strain sensors," *Sci. Rep.*, vol. 2, Nov. 2012, Art. no. 870, doi: 10.1038/srep00870.

[25] M. Gamil, O. Tabata, K. Nakamura, A. M. R. F. El-Bab, and A. A. El-Moneim, "Investigation of a new high sensitive micro-electromechanical strain gauge sensor based on graphene piezoresistivity," *Key Eng. Mater.*, vol. 605, pp. 207–210, Apr. 2014, doi: 10.4028/www.scientific.net/KEM.605.207.

[26] T. Helbling, C. Roman, L. Durrer, C. Stampfer, and C. Hierold, "Gauge factor tuning, long-term stability, and miniaturization of nanoelectromechanical carbon-nanotube sensors," *IEEE Trans. Electron Devices*, vol. 58, no. 11, pp. 4053–4060, Nov. 2011, doi: 10.1109/TED.2011.2165544.

[27] H.-P. Phan, D. V. Dao, K. Nakamura, S. Dimitrijev, and N.-T. Nguyen, "The piezoresistive effect of SiC for MEMS sensors at high temperatures: A review," *J. Microelectromech. Syst.*, vol. 24, no. 6, pp. 1663–1677, Dec. 2015, doi: 10.1109/JMEMS.2015.2470132.

[28] D. G. Senesky, B. Jamshidi, K. B. Cheng, and A. P. Pisano, "Harsh environment silicon carbide sensors for health and performance monitoring of aerospace systems: A review," *IEEE Sensors J.*, vol. 9, no. 11, pp. 1472–1478, Nov. 2009, doi: 10.1109/JSEN.2009.2026996.

[29] K.-S. Kim and G.-S. Chung, "Novel optical hydrogen sensors based on 3C–SiC membrane and photovoltaic detector," *Sens. Actuators B, Chem.*, vol. 193, pp. 42–45, Mar. 2014, doi: 10.1016/j.snb.2013.10.079.

[30] T. Dinh, D. V. Dao, H.-P. Phan, L. Wang, A. Qamar, N.-T. Nguyen, P. Tanner, and M. Rybachuk, "Charge transport and activation energy of amorphous silicon carbide thin film on quartz at elevated temperature," *Appl. Phys. Exp.*, vol. 8, no. 6, p. 061303, 2015, doi: 10.7567/APEX.8.061303.

[31] D. V. Dao, H.-P. Phan, A. Qamar, and T. Dinh, "Piezoresistive effect of p-type single crystalline 3C–SiC on (111) plane," *RSC Adv.*, vol. 6, no. 26, pp. 21302–21307, 2016, doi: 10.1039/C5RA28164D.

[32] R. Shao, K. Zheng, Y. Zhang, Y. Li, Z. Zhang, and X. Han, "Piezoresistance behaviors of ultra-strained SiC nanowires," *Appl. Phys. Lett.*, vol. 101, no. 23, p. 233109, 2012, doi: 10.1063/1.4769217.

[33] F. Gao, J. Zheng, M. Wang, G. Wei, and W. Yang, "Piezoresistance behaviors of p-type 6H–SiC nanowires," *Chem. Commun.*, vol. 47, no. 43, pp. 11993–11995, 2011, doi: 10.1039/C1CC14343C.

[34] J. Bi, G. Wei, L. Wang, F. Gao, J. Zheng, B. Tang, and W. Yang, "Highly sensitive piezoresistance behaviors of n-type 3C–SiC nanowires," *J. Mater. Chem. C*, vol. 1, no. 30, pp. 4514–4517, 2013, doi: 10.1039/C3TC30655K.

[35] H.-P. Phan, A. Qamar, D. V. Dao, T. Dinh, L. Wang, J. Han, P. Tanner, S. Dimitrijev, and N.-T. Nguyen, "Orientation dependence of the pseudo-Hall effect in p-type 3C–SiC four-terminal devices under mechanical stress," *RSC Adv.*, vol. 5, no. 69, pp. 56377–56381, 2015, doi: 10.1039/C5RA10144A.

[36] A. Qamar, H.-P. Phan, J. Han, P. Tanner, T. Dinh, L. Wang, S. Dimitrijev, and D. V. Dao, "The effect of device geometry and crystal orientation on the stress-dependent offset voltage of 3C–SiC(100) four terminal devices," *J. Mater. Chem. C*, vol. 3, no. 34, pp. 8804–8809, 2015, doi: 10.1039/C5TC01898F.

[37] T. Dinh, H.-P. Phan, T. Kozeki, A. Qamar, T. Namazu, N.-T. Nguyen, and D. V. Dao, "Thermoresistive properties of p-type 3C–SiC nanoscale thin films for high-temperature MEMS thermal-based sensors," *RSC Adv.*, vol. 5, no. 128, pp. 106083–106086, 2015, doi: 10.1039/C5RA20289B.

[38] P. Tanner, L. Wang, S. Dimitrijev, J. Han, A. Iacopi, L. Hold, and G. Walker, "Novel electrical characterization of thin 3C–SiC films on Si substrates," *Sci. Adv. Mater.*, vol. 6, no. 7, pp. 1542–1547, 2014, doi: 10.1166/sam.2014.1813.

[39] X. Gao, W.-H. Shih, and W. Y. Shih, "Induced voltage of piezoelectric unimorph cantilevers of different nonpiezoelectric/piezoelectric length ratios," *Smart Mater. Struct.*, vol. 18, no. 12, p. 125018, 2009, doi: 10.1088/0964-1726/18/12/125018.

[40] T. Toriyama, Y. Tanimoto, and S. Sugiyama, "Single crystal silicon nano-wire piezoresistors for mechanical sensors," *J. Microelectromech. Syst.*, vol. 11, no. 5, pp. 605–611, Oct. 2002, doi: 10.1109/JMEMS.2002.802905.